Coptisine prevents angiotensin II-induced endothelial cell injury and senescence via the lncRNA SNHG12/miR-603/NAMPT pathway

JING MENG, XIAOYING SONG, XINYUE XING, JINGYI CHEN and DANFEI LOU

Emergency Department, Shanghai Municipal Hospital of Traditional Chinese Medicine, Shanghai University of Traditional Chinese Medicine, Shanghai 200071, P.R. China

Received July 22, 2023; Accepted November 23, 2023

DOI: 10.3892/etm.2023.12356

Abstract. Atherosclerosis (AS) is a major health problem and targeting the associated molecular pathways is critical for developing therapies. The present study investigated the effect of coptisine on human umbilical vein endothelial cells (HUVECs) in response to angiotensin II (Ang II) induction by focusing on cellular senescence, apoptosis and inflammation. HUVECs were treated with different Ang II concentrations and long non-coding RNA small nucleolar RNA host gene 12 (SNHG12), microRNA (miRNA/miR)-603 and nicotinamide phosphoribosyltransferase (NAMPT) expressions were assessed. Cell viability, nicotinamide adenine dinucleotide (NAD+) levels, senescence, apoptosis and inflammation were assessed. The interactions among SNHG12, miR-603 and NAMPT were investigated using dual-luciferase reporter gene assays and RNA pull-down experiments. Coptisine treatment increased SNHG12 expression and attenuated Ang II-induced adverse effects in HUVECs. SNHG12 silencing abrogated coptisine's protective effects, indicating that SNHG12 is a key mediator. SNHG12 targets miR-603, which then directly targets NAMPT, an age-related gene involved in NAD(+) regulation. Coptisine modulated the SNHG12/miR-603/NAMPT pathway and miR-603 inhibition enhanced the protective effects of coptisine. NAMPT overexpression reversed the negative effects of miR-603 and enhanced the protective effect of the miR-603 inhibitor. Finally, the protective mechanism of coptisine is linked to the regulation of NAD(+), sirtuin 3 (SIRT3) and p53. Coptisine treatment counteracted the AngII-induced increase in SIRT3 and p53 protein levels, whereas the miR-603 inhibitor potentiated the effect of coptisine. SNHG12 knockdown partially abolished these effects, which were reversed by NAMPT overexpression. In conclusion, the present study revealed a novel protective mechanism involving the SNHG12/miR-603/NAMPT pathway in HUVECs exposed to Ang II, highlighting the potential therapeutic application of coptisine in treating atherosclerosis. These results suggested that coptisine exerts its protective effects by modulating the SNHG12/miR-603/NAMPT axis, which ultimately affects the regulation of NAD(+), SIRT3 and p53. Future studies should explore the potential of the SNHG12/miR-603/NAMPT pathway as a target for developing novel AS therapies.

Correspondence to: Dr Danfei Lou, Emergency Department, Shanghai Municipal Hospital of Traditional Chinese Medicine, Shanghai University of Traditional Chinese Medicine, 274 Middle Zhijiang Road, Jing'an, Shanghai 200071, P.R. China
E-mail: drldf123@163.com

Abbreviations: AS, atherosclerosis; HUVECs, human umbilical vein endothelial cells; lncRNA, long non-coding RNA; miR/miRNA, microRNA; siRNA, short interfering RNA; NAMPT, nicotinamide phosphoribosyltransferase; NAD, nicotinamide adenine dinucleotide; SIRT3, sirtuin 3; β-Gal, β-Galactosidase; NC, negative control; PBS, phosphate-buffered saline; ELISA, enzyme-linked immunosorbent assay; RT-qPCR, reverse transcription-quantitative polymerase chain reaction; SNHG12, small nucleolar RNA host gene 12; ov-NAMPT, over expressed NAMPT; IL, interleukin; TNF-α, tumor necrosis factor-α

Key words: atherosclerosis, cellular senescence, coptisine, long non-coding RNA small nucleolar RNA host gene 12, microRNA 603, nicotinamide phosphoribosyltransferase

Introduction

Atherosclerosis (AS), an important factor in cardiovascular disease, is characterized by the buildup of lipids, immune cells and extracellular matrix elements in the vascular intima, resulting in plaque development and vascular remodeling (1,2). Senescence-associated secretory phenotype, a proinflammatory phenotype that contributes to the chronic inflammatory milieu within atherosclerotic plaques, has emerged as a key factor in AS onset and progression (3,4). Cellular senescence causes the malfunction of endothelial cells in blood vessels (5). Targeting cellular senescence could be a potential treatment strategy for AS and its associated side effects.

Coptisine is a bioactive alkaloid compound that is primarily found in various plant species, especially those in the *Coptis* genus in the family Ranunculaceae, which have been reported to exhibit various pharmacological effects, including anti-inflammatory, anti-oxidant and anti-atherosclerotic properties (6,7). Previous studies have demonstrated the

potential of coptisine to ameliorate endothelial dysfunction and inhibit vascular smooth muscle cell proliferation (8,9). Additionally, coptisine exerts protective effects against cellular senescence (10). Although no studies have confirmed the effect of coptisine on endothelial cell senescence, such as in human umbilical vein endothelial cells (HUVECs), which are commonly used in *in vitro* cell models of AS in the presence of angiotensin II (Ang II), its antioxidative and anti-inflammatory properties indicates its potential anti-aging role in these cells. This finding warrants further in-depth investigation of the underlying mechanisms.

Accumulating evidence suggests that long non-coding RNAs (lncRNAs) and microRNAs (miRNAs) play crucial roles in regulating cellular senescence and AS (11). Particularly, lncRNAs can function as competing endogenous RNAs that sponge miRNAs, thereby modulating the expression of miRNA target genes and influencing cellular processes relevant to AS (12). The lncRNA small nucleolar RNA host gene 12 (SNHG12) is downregulated in AS and is an effective AS inhibitor (13). Studies on miR-603 have focused on its effects on tumor growth (14,15). However, because of its effects on inflammation (14), it was hypothesized that it may regulate AS.

Nicotinamide phosphoribosyltransferase (NAMPT) is a key enzyme involved in the biosynthesis of nicotinamide adenine dinucleotide (NAD+), a crucial coenzyme in cellular energy metabolism and redox reactions (16). Altered NAD(+) homeostasis has been implicated in the development of age-related diseases, including AS (17). Sirtuin 3 (SIRT3) is an NAD+-dependent protein deacetylase that removes acetyl groups from other proteins in the presence of the coenzyme NAD+ (18) and regulates cellular processes such as inflammation, oxidative stress and apoptosis (19,20) by deacetylating target proteins, including p53 (21). The NAD(+)/SIRT3/p53 signaling axis has been implicated in endothelial function regulation and AS development (22); however, its potential involvement in the protective effects of coptisine remains to be elucidated.

In summary, the present study highlighted the importance of coptisine as a potential therapeutic agent for combating AS and its associated complications by targeting cellular senescence. Identifying the SNHG12/miR-603/NAMPT axis as a critical mediator of the anti-senescence effects of coptisine provides a novel target for future therapeutic interventions and broadens our understanding of the molecular mechanisms governing endothelial cell function and dysfunction in AS.

Materials and methods

Cell culture, treatment and transfection. HUVECs were purchased from ATCC and cultured in endothelial cell growth medium (Procell Life Science & Technology Co., Ltd.) supplemented with 10% fetal bovine serum (Gibco; Thermo Fisher Scientific, Inc.). Cells were maintained at 37˚C and 5% CO_2. HUVECs were exposed to different concentrations of coptisine (MilliporeSigma) dissolved in dimethyl sulfoxide (MilliporeSigma) for 24 h at 37˚C. Coptisine at 0-100 μM in HUVECs for 24 h at 37˚C was used to assay the effect of coptisine itself on cell viability. HUVECs were pre-treated with 6.25 (low-dose, L), 12 (medium-dose, M) and 25 μM (high-dose, H) coptisine for 6 h before Ang II treatment. After pre-treatment, cells were exposed to 1 μM Ang II in the presence of coptisine for an additional 24 or 48 h at 37˚C. SNHG12 small interfering (si)RNAs, miR-603 mimic/inhibitor and NAMPT overexpression vector (ov-NAMPT) constructed using the pCMV6-Entry backbone and their negative controls (NCs) were from Guangzhou RiboBio Co., Ltd. and were transfected into HUVECs using Lipofectamine® 3000 (Invitrogen; Thermo Fisher Scientific, Inc.) for 4 h and continued in culture at 37˚C for 24 or 48 h after fresh medium change. The si-SNHG12, miRNAs and their NC sequences used were as follows: si-SNHG12-1, CTTTAAGATTCATGT TACATT; si-SNHG12-2, GGGTAATGACAGTGATGAATT; si-SNHG12-3, GGATGACTGACTTAGTCTATT; si-NC, TTG TACTACACAAAAGTACTG; miR-603 mimic, CACACA CTGCAATTACTTTTGC; mimic NC, ACTGTACCACAG TTTCCCTTAA; miR-603 inhibitor, GCAAAAGTAATT GCAGTGTGTG; and inhibitor NC, CAGTACTTTTGTGTA GTACAA.

Cell viability assay. Following the manufacturer's instructions, HUVECs were cultured for 24 h and incubated for 60 min with 10 ml Cell Counting Kit-8 (CCK8; Beijing Solarbio Science & Technology Co., Ltd.) reagent every 24 h for 48 h at 37˚C. Optical density was determined using a spectrophotometer (Thermo Fisher Scientific, Inc.).

Senescence-associated β-galactosidase (β-Gal) staining. A senescence-associated β-Gal staining kit (Beyotime Institute of Biotechnology) was used to measure cellular senescence in accordance with the manufacturer's instructions. HUVECs were seeded in 6-well plates and treated as previously described. Following treatment, cells were rinsed with phosphate-buffered saline (PBS), fixed for 15 min with 4% paraformaldehyde at 21˚C and then stained overnight at 37˚C. A light microscope (Olympus Corporation) was used to count the blue-stained cells and calculate the proportion of senescent cells.

Apoptosis detection. The Annexin V-FITC/propidium iodide (PI) apoptosis detection kit (BD Biosciences) was used to measure apoptosis. Following treatment, the HUVECs were rinsed with cold PBS and resuspended in a binding buffer. The cells were treated with PI and Annexin V-FITC for 15 min at 21˚C in the dark. Flow cytometry (BD FACSCalibur™ flow cytometer; BD Biosciences) was used to investigate apoptosis and the FlowJo software (version 10.6.2; FlowJo LLC) was used to calculate the percentage of early + late apoptotic cells.

NAD(+)/NADH (H for hydrogen) analysis. Following the manufacturer's instructions, after microglia were lysed using the extract, the NAD(+)/NADH ratio was measured using an NAD(+) kit (Beyotime Institute of Biotechnology). The extraction solution was used to construct a standard curve. The sample and enzyme working solution were added to the 96-well plate, incubated at 37˚C and the chromogenic agent was added for further incubation. A spectrophotometer (UV-8000A; Shanghai Metash Instruments Co., Ltd.) was used to measure absorbance at 450 nm.

Enzyme-linked immunosorbent assay (ELISA). Inflammatory markers, including interleukin-1 β (IL-1β; cat. no. SLB50), IL-6 (cat. no. S6050) and tumor necrosis factor-α (TNF-α; cat. no. STA00D) were measured using ELISA kits (R&D Systems, Inc.) following the manufacturer's instructions. After treatment, cell culture supernatants were collected and centrifuged at 1,000 x g for 5 min at 21˚C to remove debris. The supernatants were then used for ELISA and the absorbance was measured at 450 nm using a microplate reader (BioTek Instruments, Inc.). The concentrations of the inflammatory markers were calculated based on standard curves.

Nucleocytoplasmic separation experiments. HUVECs were harvested and washed with cold PBS. The cells were then resuspended in a hypotonic buffer containing 10 Tris-HCl (pH 7.4), 10 NaCl and 3 mM $MgCl_2$. After a 10-min incubation on ice, 10% NP-40 (MilliporeSigma) was added to the cell suspension, followed by vortexing for 10 sec. The cell lysate was centrifuged at 3,000 x g for 10 min at 4˚C. The supernatant, which contained the cytoplasmic fraction, was carefully transferred to a new tube. The pellet, which contains the nuclear fraction, was washed with the hypotonic buffer to remove any remaining cytoplasmic contaminants. Total RNA from both the cytoplasmic and nuclear fractions was extracted using the TRIzol® reagent (Thermo Fisher Scientific, Inc.), following the manufacturer's instructions. Cytoplasmic and nuclear RNA were isolated from HUVECs for reverse transcription-quantitative polymerase chain reaction (RT-qPCR) analysis using a cytoplasmic and nuclear RNA purification kit (Norgen Biotek Corp.).

RT-qPCR assay. Total RNA was isolated from HUVECs ($1x10^6$) using TRIzol reagent (Thermo Fisher Scientific, Inc.), following the manufacturer's instructions. The RNA concentration and purity were measured using a NanoDrop spectrophotometer (Thermo Fisher Scientific) according to the manufacturer's instructions. A High-Capacity complementary DNA Reverse Transcription Kit (Applied Biosystems) was used to generate complementary DNA according to the manufacturer's instructions. On the Applied Biosystems 7500 Real-Time PCR System (Applied Biosystems), RT-qPCR was carried out using the Power SYBR Green PCR Master Mix (Applied Biosystems) according to the manufacturer's instructions. PCR amplification was performed under the following conditions: 95˚C for an initial 30 sec, followed by 40 cycles at 95˚ for 5 sec and 60˚C for 30 sec. The relative expression of target genes was calculated using the $2^{-\Delta\Delta Cq}$ method (23) and normalized to the expression of β-actin or U6 small nuclear RNA as internal controls. The primer sequences used were as follows: SNHG12 forward, 5'-ACAGGCGGATAAAACGGTCC-3' and reverse, 5'-AGTACGCCGGGATCTCTGTA-3'; miR-603 forward, 5'-ACACTCCAGCTGGGCACACACTGCAATTAC-3' and reverse, 5'-CTCAACTGGTGTCGTGGA-3'; NAMPT forward, 5'-ACCATAACAGCTTGGGGGAA-3' and reverse, 5'-CTGACCACAGATACAGGCAC-3'; β-actin forward, 5'-AGCGAGCATCCCCCAAAGTT-3' and reverse, 5'-GGGCACGAAGGCTCATCATT-3'; and U6 forward, 5'-CTCGCTTCGGCAGCACA-3' and reverse, 5'-AACGCTTCACGAATTTGCGT-3'. These experiments were repeated three times.

Binding site analysis and dual-luciferase reporter gene assay. The LncBase v 3.0 (https://diana.e-ce.uth.gr/lncbasev3/interactions) and miRanda v3.3a (http://www.microrna.org/) were used to analyze the potential binding sites between lncRNA and miRNA, and themiRDB (https://mirdb.org/) database was used to identify the downstream targets of miRNA. Interactions between miR-603 with NAMPT mRNA 3'UTR and SNHG12 were investigated using the dual-luciferase reporter gene assay. HUVECs were co-transfected with miR-603 mimic or mimic NC and either wild type (WT) or mutant (mut) NAMPT 3'UTR or SNHG12 reporter plasmids using Lipofectamine® 3000. The plasmids were synthesized by Guangzhou RiboBio Co., Ltd., and inserted into psiCHECK™-2 vector plasmids (Promega Corporation), and pRL-SV40 reporter vector plasmids (Promega Corporation) were acquired. After 48 h, the lysed cells were used to assess luciferase activity using a Dual-Luciferase Reporter Assay System (Promega Corporation) and GloMax Luminometer (Promega Corporation). To increase transfection effectiveness, firefly luciferase activity was normalized to *Renilla* luciferase activity.

RNA pull-down assay. The interaction between SNHG12 and miR-603 was assessed using an RNA pull-down assay. Biotinylated miR-603 mimics and biotinylated NC mimics were synthesized by Guangzhou RiboBio Co., Ltd. The plasmid backbone employed was pcDNA3.1 (Guangzhou RiboBio Co., Ltd.) used at a concentration of 100 ng/μl. HUVECs were lysed and incubated (4˚C) with the biotinylated RNA probes for 2 h. Following this, 50 μl streptavidin agarose beads (Thermo Fisher Scientific, Inc.) was added to the mixture and incubation continued for an additional 2 h at 4˚C. The centrifugation steps were conducted at 1,000 x g for 5 min at 4˚C, both after the initial incubation and following the addition of the beads. After these steps, the beads were washed and the bound RNAs were extracted using the PureLink RNA Mini Kit (Invitrogen; Thermo Fisher Scientific, Inc.) according to the manufacturer's instructions. The beads were washed and the bound RNAs were extracted using TRIzol (Thermo Fisher Scientific, Inc.) for RT-qPCR analysis.

Western blotting. HUVECs were lysed using RIPA buffer (Beyotime Institute of Biotechnology). The protein concentration in the sample was measured using a bicinchoninic acid kit (Beyotime Institute of Biotechnology). Proteins (20 μg) were separated by SDS-PAGE on 10% gels and transferred to polyvinylidene fluoride membranes (MilliporeSigma), before being blocked with 5% bovine serum albumin for 1 h at 21˚C (Thermo Fisher Scientific, Inc.) and incubated with primary antibodies against NAMPT (1:1,000; MA5-24108; Invitrogen), SIRT3 (1:1,000; ab217319; Abcam), p53 (1:1,000; ab32049; Abcam) and β-actin (1:1,000; ab8227; Abcam) overnight at 4˚C. The membranes were washed and then incubated for 1 h at 21˚C with horseradish peroxidase-conjugated secondary antibodies (1:5,000; ab97051; Abcam). An enhanced chemiluminescence substrate was used to detect the protein bands and a ChemiDoc XRS+ imaging system (Bio-Rad Laboratories, Inc.) was used for visualization. Gray values were quantified using ImageJ software (National Institutes of Health). NAMPT,

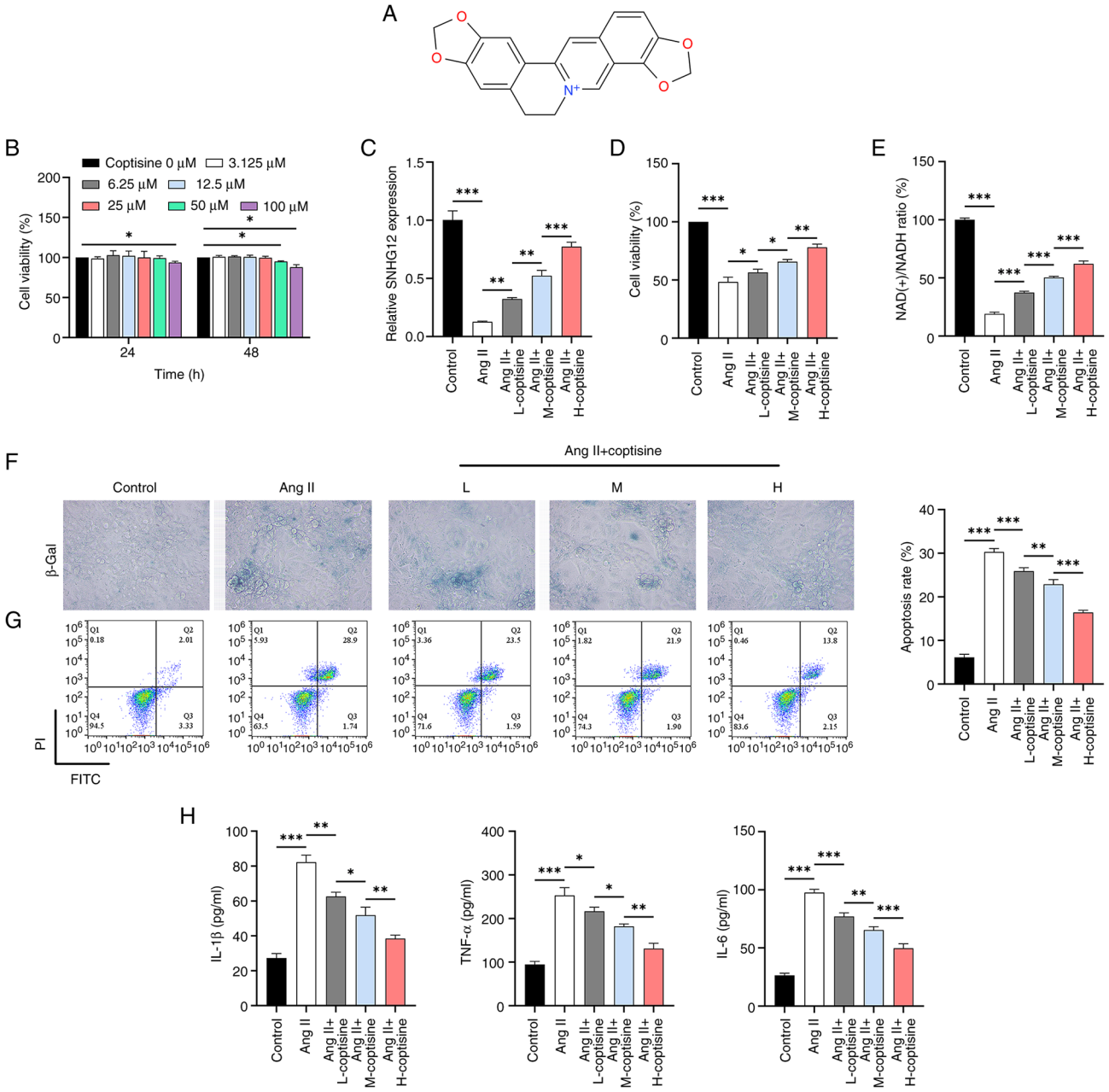

Figure 1. Evaluation of the effects of SNHG12 and varying coptisine concentrations on HUVECs. (A) Chemical structure of coptisine. (B) CCK8 assay analyzing the impact of different doses of coptisine on the viability of HUVECs. (C) RT-qPCR analysis evaluating the influence of various coptisine doses on SNHG12 expression under Ang II induction. (D) CCK8 assay exploring the effects of different coptisine doses on HUVEC viability following Ang II induction. (E) NAD(+) assay kit used to determine the NAD(+)/NADH ratio. (F) β-Gal assay analyzing the effects of coptisine on cellular senescence in HUVECs induced by Ang II. Magnification, x400. (G) Flow cytometry examining the effect of coptisine on apoptosis in HUVECs induced by Ang II. (H) ELISA investigation of the influence of coptisine on the inflammatory cytokine levels (IL-1β, TNF-α and IL-6) in HUVECs following Ang II induction. *P<0.05, **P<0.01 and ***P<0.001. SNHG12, small nucleolar RNA host gene 12; HUVECs, human umbilical vein endothelial cells; CCK8, Cell Counting Kit-8; RT-qPCR, real-time quantitative polymerase chain reaction; Ang II, angiotensin II; NAD, nicotinamide adenine dinucleotide; β-Gal, β-galactosidase; ELISA, enzyme-linked immunosorbent assay; IL, interleukin; TNF-α, tumor necrosis factor-α; L, 6.25 μM; M,12 μM; H, 25 μM.

SIRT3 and p53 protein levels were adjusted to β-actin as the internal reference.

Statistical analysis. All experiments were performed at least three times and data were presented as mean ± standard deviation. Statistical analyses were performed using GraphPad Prism 9 software (GraphPad Software; Dotmatics). Comparisons between groups were conducted using one-way analysis of variance, followed by Tukey's post hoc test. P<0.05 was considered to indicate a statistically significant difference.

Results

Investigation of the role of SNHG12 and coptisine concentrations. Initially, at different coptisine concentrations (Fig. 1A), HUVECs showed a slight decrease in activity start at a concentration of 50 μM (Fig. 1B). Concentrations of 6.25, 12 and 25 μM (48 h) were chosen for subsequent experiments because they did not have a significant effect on cell viability. The results showed a decrease in SNHG12 expression upon Ang II induction, whereas coptisine treatment at different

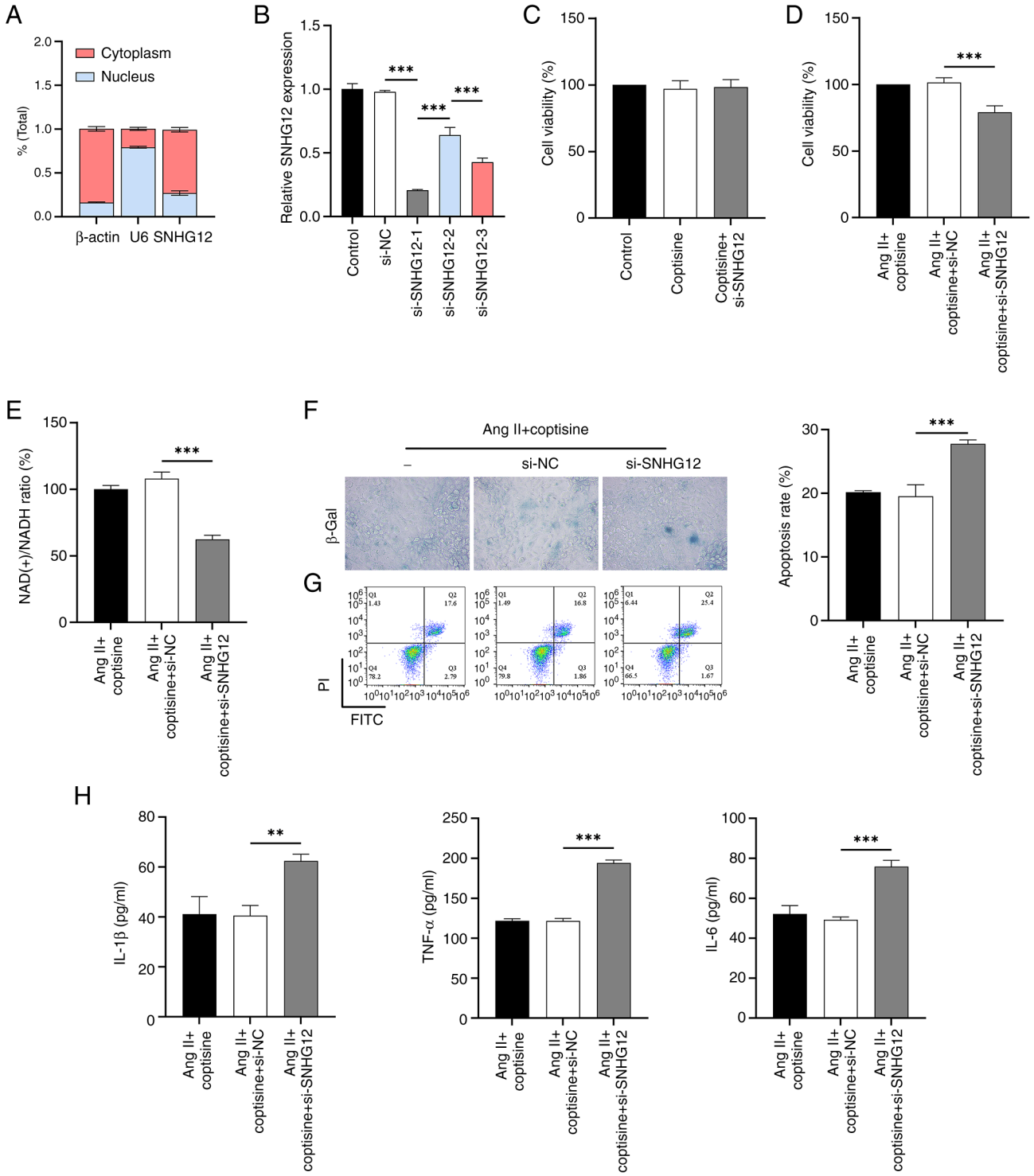

Figure 2. SNHG12 pathway mediated anti-senescence and anti-apoptosis effects of coptisine. (A) Nuclear cytoplasmic separation experiment analyzing subcellular localization of SNHG12. (B) RT-qPCR analysis of the inhibition efficiency of three siRNAs targeting SNHG12. CCK8 assay assessing the influence of si-SNHG12 on the viability of HUVECs induced by (C) coptisine or/and (D) Ang II. (E) NAD(+) assay kit determining the NAD(+)/NADH ratio in HUVECs induced by Ang II and treated with si-SNHG12. (F) β-Gal assay exploring the effects of si-SNHG12 on cellular senescence in HUVECs induced by Ang II. Magnification, x400. (G) Flow cytometry analyzing the impact of si-SNHG12 on apoptosis in HUVECs induced by Ang II. (H) ELISA investigation of the influence of si-SNHG12 on inflammatory cytokine levels (IL-1β, TNF-α and IL-6) in HUVECs induced by Ang II. **P<0.01 and ***P<0.001. SNHG12, small nucleolar RNA host gene 12; RT-qPCR, real-time quantitative polymerase chain reaction; siRNA, short interfering RNA; HUVECs, human umbilical vein endothelial cells; CCK8, Cell Counting Kit-8; Ang II, Angiotensin II; β-Gal, β-galactosidase; NAD, nicotinamide adenine dinucleotide; ELISA, enzyme-linked immunosorbent assay; IL, interleukin; TNF-α, tumor necrosis factor-α.

concentrations induced a dose-dependent increase in SNHG12 expression (Fig. 1C). Meanwhile, Ang II induction resulted in decreased cell viability (Fig. 1D) and NAD(+)/NADH ratio (Fig. 1E), as well as increased levels of senescence (Fig. 1F), apoptosis (Fig. 1G) and inflammation (increased IL-1β, IL-6 and TNF-α; Fig. 1H). Treatment with coptisine attenuated the

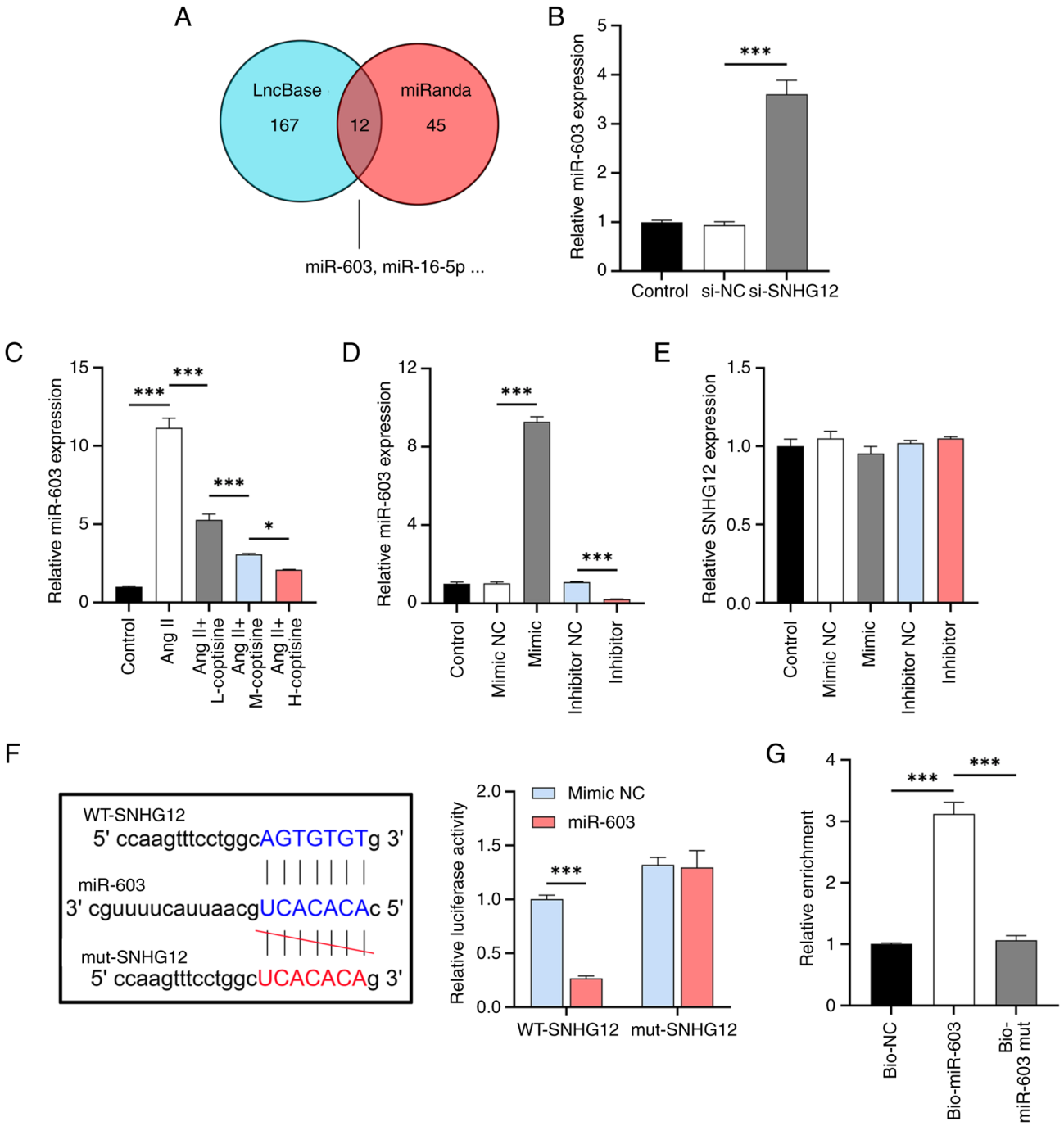

Figure 3. LncRNA SNHG12 as a molecular sponge for miR-603. (A) Joint analysis of LncBase and miRanda databases for potential target miRNAs of lncRNA SNHG12. (B) RT-qPCR analysis of the effect of si-SNHG12 on miR-603 expression. (C) RT-qPCR analysis assessing the effects of coptisine on miR-603 expression in HUVECs induced by Ang II. (D) RT-qPCR validation of miR-603 mimic/inhibitor in HUVECs. (E) RT-qPCR analysis of the effect of miR-603 expression changes on SNHG12 expression. (F) Dual-luciferase reporter gene assay determining the binding between SNHG12 and miR-603. (G) RNA pull-down experiment analyzing SNHG12 enrichment in the bio-miR-603 group. *P<0.05 and ***P<0.001. lncRNA, long non-coding RNA; SNHG12, small nucleolar RNA host gene 12; miR, microRNA; RT-qPCR, real-time quantitative polymerase chain reaction; HUVECs, human umbilical vein endothelial cells; bio, biotinylated; Ang II, Angiotensin II; L, 6.25 μM; M,12 μM; H, 25 μM; mut, mutant; WT, wild type; NC, negative control.

effects of Ang II induction, with the improvements becoming more pronounced as coptisine concentration increased.

Coptisine inhibits cell senescence and apoptosis via the SNHG12 pathway. The results of nucleoplasmic segregation experiments showed that, consistent with the positive control β-actin and in contrast to the positive control U6, lncRNA SNHG12 was mainly expressed in the cytoplasm of HUVECs (Fig. 2A). For silencing SNHG12 expression, si-SNHG12-1 was selected for optimal inhibition efficiency (Fig. 2B). It was found that SNHG12 knockdown had no significant effect on the activity of coptisine (25 μM)-treated HUVECs (Fig. 2C). Subsequent results showed that SNHG12 interference counteracted the protective effects of coptisine against Ang II-induced decreases in cell viability (Fig. 2D) and NAD(+)/NADH ratio (Fig. 2E), as well as increased senescence (Fig. 2F), apoptosis

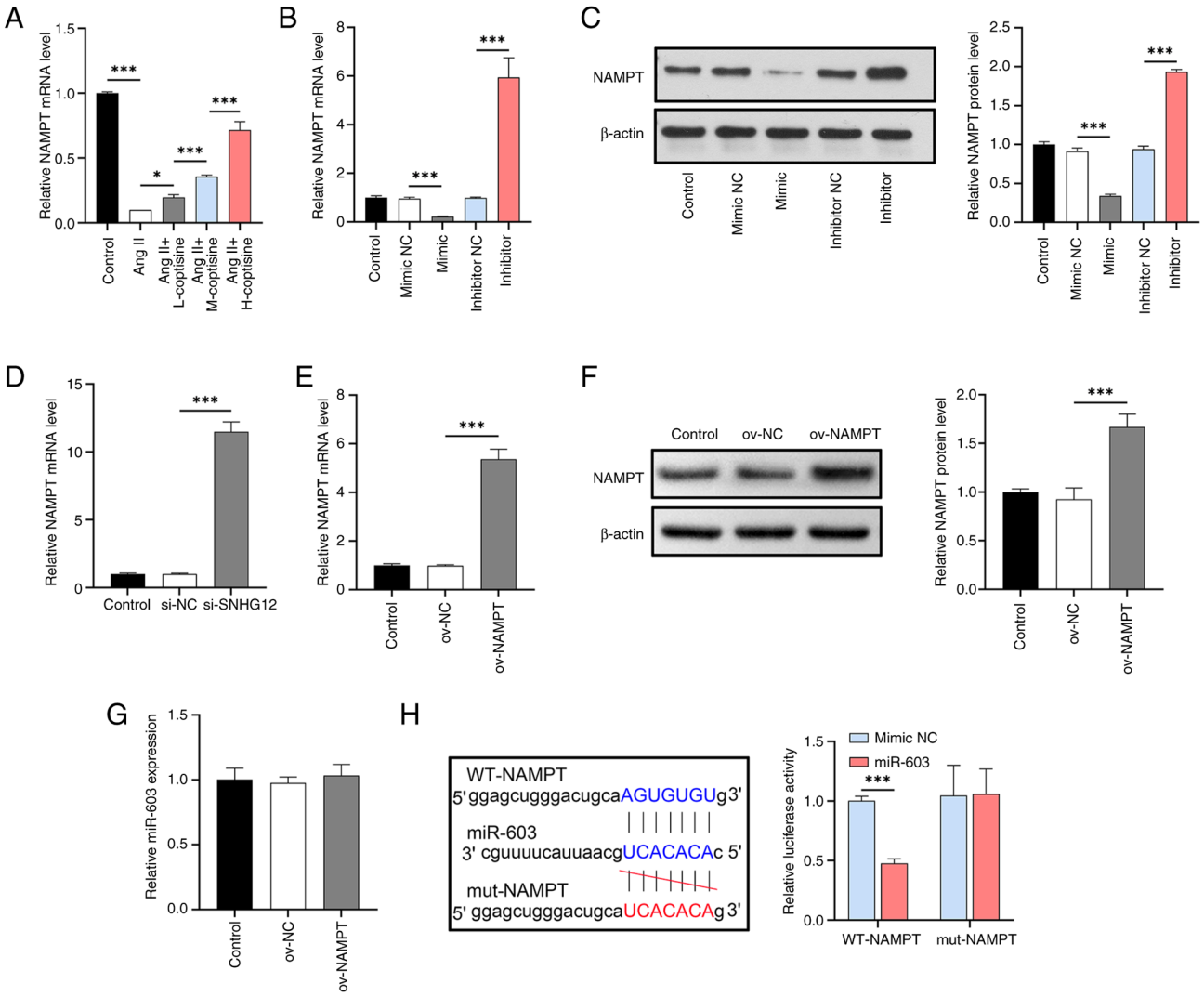

Figure 4. NAMPT identified as a direct target of miR-603. (A) RT-qPCR analysis examining the influence of coptisine on NAMPT expression in HUVECs induced by Ang II. (B) RT-qPCR analysis assessing the impact of miR-603 mimic/inhibitor on NAMPT expression. (C) Western blot analysis assessing the impact of miR-603 mimic/inhibitor on NAMPT protein level. (D) RT-qPCR analysis evaluating the effects of si-SNHG12 on NAMPT expression. (E) RT-qPCR analysis verifying the efficacy of the NAMPT overexpression vector. (F) Western blot analysis confirms the functionality of the NAMPT overexpression vector. (G) RT-qPCR analysis determining the influence of the NAMPT overexpression vector on miR-603 expression. (H) Dual-luciferase reporter gene assay confirming the binding between NAMPT and miR-603. *P<0.05 and ***P<0.001. NAMPT, Nicotinamide phosphoribosyltransferase; miR, microRNA; RT-qPCR, real-time quantitative polymerase chain reaction; HUVECs, human umbilical vein endothelial cells; Ang II, Angiotensin II; ov, overexpression; mut, mutant; WT, wild type; NC, negative control.

(Fig. 2G) and inflammation (Fig. 2H). The maximum safe concentration for coptisine dose selection was 25 μM.

lncRNA SNHG12 acts as a molecular sponge to absorb miR-603. To investigate the mechanism of action of SNHG12, the target miRNAs of SNHG12 (Fig. 3A) were identified using the LncBase and miRanda databases and 12 miRNAs with potential binding sites to SNHG12 were identified. A literature search revealed that only one miRNA, miR-603, has not been reported in AS and its expression was increased by si-SNHG12 (Fig. 3B) and Ang II induction but inhibited by coptisine in a dose-dependent manner (Fig. 3C). After validating the efficacy of the miR-603 mimic/inhibitor in HUVECs (Fig. 3D), no significant effect of its expression changes on lncRNA SNHG12 was observed (Fig. 3E). Furthermore, WT SNHG12 cotransfected with the miR-603 mimic showed significantly lower fluorescence activity compared to the cotransfected mimic NC, as determined by the dual luciferase reporter gene assay. By contrast, the fluorescence intensity of the miR-603 mimic or mimic NC cotransfected with mut SNHG12 did not change significantly (Fig. 3F). RNA pull-down experiments showed that SNHG12 was enriched in miR-603 precipitation compared to the control, further supporting their interaction (Fig. 3G). These results indicated that miR-603 was a direct SNHG12 target.

NAMPT is a direct target of miR-603. To further understand the mechanism of SNHG12/miR-603, the miRDB database was used to identify the downstream targets of miR-603. Among the mRNAs with potential binding sites, NAMPT is a known age-related gene and its activation significantly promotes the NAD(+)/NADH ratio (24). The present study showed that Ang II induction reduced NAMPT expression, whereas treatment with different coptisine

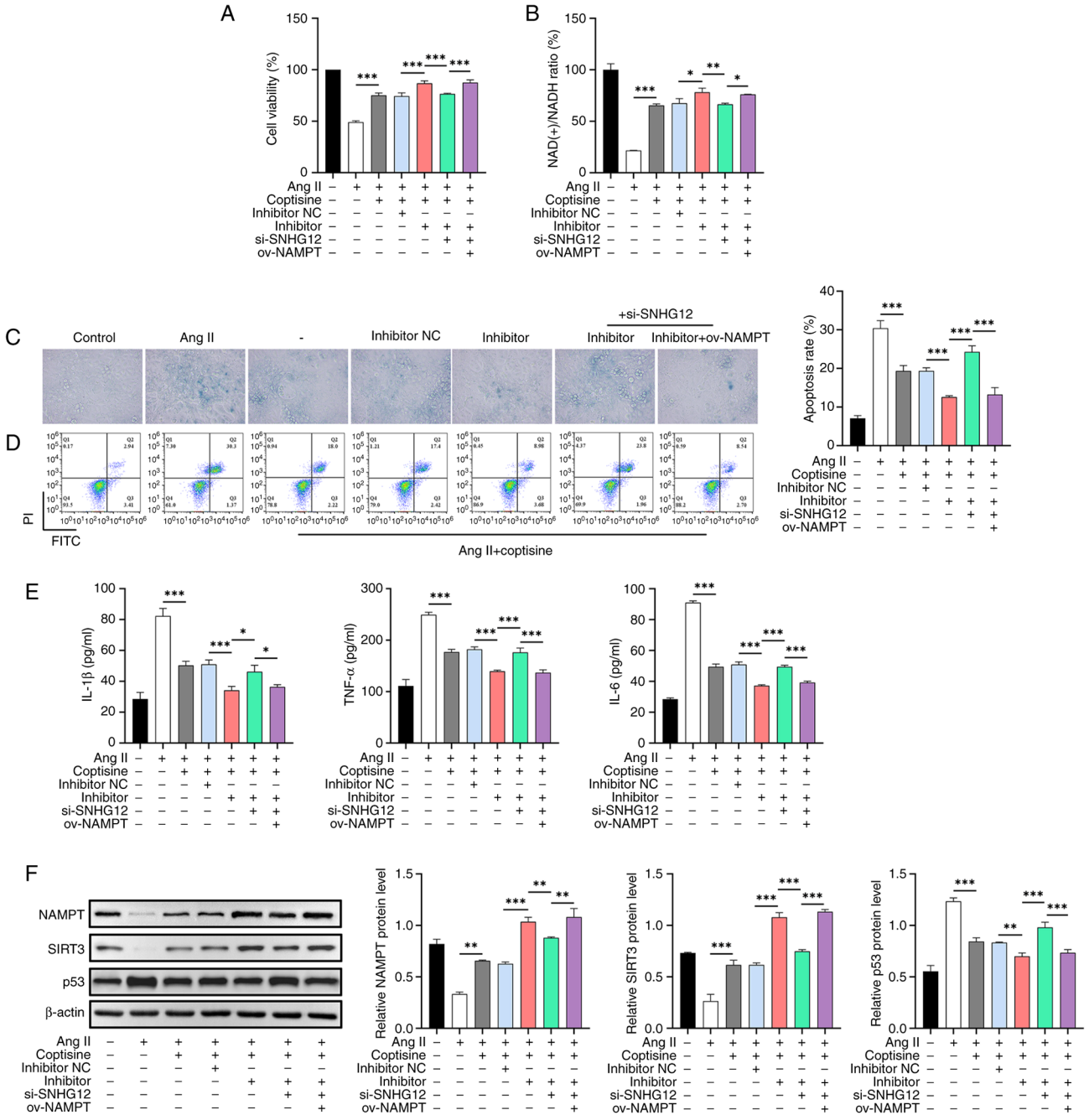

Figure 5. The role of the SNHG12/miR-603/NAMPT axis in protective mechanism of coptisine. (A) CCK8 assay analyzing the effect of the SNHG12/miR-603/NAMPT axis on the viability of HUVECs induced by Ang II. (B) NAD(+) assay kit determining the NAD(+)/NADH ratio in HUVECs induced by Ang II and influenced by the SNHG12/miR-603/NAMPT axis. (C) β-Gal assay examining the effects of the SNHG12/miR-603/NAMPT axis on cellular senescence in HUVECs induced by Ang II. Magnification, x400. (D) Flow cytometry analyzing the impact of the SNHG12/miR-603/NAMPT axis on apoptosis in HUVECs induced by Ang II. (E) ELISA investigation of the influence of the SNHG12/miR-603/NAMPT axis on the inflammatory cytokine levels (IL-1β, TNF-α and IL-6) in HUVECs induced by Ang II. (F) Western blot analysis assessing the effects of the SNHG12/miR-603/NAMPT axis on the NAMPT, SIRT3 and p53 protein levels in HUVECs induced by Ang II. *P<0.05, **P<0.01 and ***P<0.001. SNHG12, small nucleolar RNA host gene 12; miR, microRNA; NAMPT, Nicotinamide phosphoribosyltransferase; ov, overexpression; CCK8, Cell Counting Kit-8; HUVECs, human umbilical vein endothelial cells; Ang II, Angiotensin II; NAD, nicotinamide adenine dinucleotide; β-Gal, β-galactosidase; ELISA, enzyme-linked immunosorbent assay; IL, interleukin; TNF-α, tumor necrosis factor-α; SIRT3, Sirtuin 3; p53, protein 53; ov, overexpression; NC, negative control.

concentrations resulted in a dose-dependent increase in NAMPT expression (Fig. 4A). Additionally, NAMPT expression and protein levels were negatively regulated by miR-603 (Fig. 4B and C) and its expression was inhibited by si-SNHG12 (Fig. 4D). Subsequent dual-luciferase detection confirmed that NAMPT was a direct target of miR-603 (Fig. 4E). Therefore, NAMPT was identified as an miR-603 target and an NAMPT overexpression vector was constructed and validated for gene and protein levels in HUVECs (Fig. 4F and G), with no significant effect on miR-603 (Fig. 4H).

SNHG12/miR-603/NAMPT is involved in the protective mechanism of coptisine. As expected, coptisine

significantly ameliorated Ang II-induced decreases in cell viability (Fig. 5A) and NAD(+)/NADH ratio (Fig. 5B), as well as increased senescence (Fig. 5C), apoptosis (Fig. 5D) and inflammation (Fig. 5E). This ameliorative effect was enhanced by the miR-603 inhibitor but was partly neutralized by si-SNHG12. Transfection with ov-NAMPT reversed the neutralizing effect of si-SNHG12. Furthermore, unlike p53 protein levels, Ang II decreased NAMPT and SIRT3 protein levels, which were partially counteracted by coptisine. The miR-603 inhibitor enhanced the effect of coptisine; however, this effect was partially abrogated by the interference with SNHG12 expression; ov-NAMPT reversed these effects (Fig. 5F).

Discussion

Currently, the primary treatment for AS involves statins to lower cholesterol levels and slow disease progression. However, potential side effects include muscle pain and liver and kidney damage (25,26). Therefore, safer and more effective therapeutic strategies are crucial. The present study aimed to explore novel treatment strategies for ameliorating AS and their underlying molecular mechanisms. It investigated the role of coptisine in HUVECs by focusing on its effects on cell viability, senescence, apoptosis and inflammation. The results showed that coptisine treatment mitigated the detrimental effects of Ang II induction in HUVECs by modulating the SNHG12/miR-603/NAMPT signaling pathway.

Ang II acting on HUVECs is a commonly used *in vitro* cellular model of AS (27,28) and this model was used to explore the potential role and mechanism of coptisine on AS and to demonstrate, for the first time to the best of the authors' knowledge, the antioxidant, anti-inflammatory and anti-aging effects of coptisine in HUVECs. These results were consistent with those of previous studies on coptisine usefulness (7,29). In parallel, SNHG12 expression increased with increasing coptisine doses, suggesting that SNHG12 may play a role in the protective effects of coptisine. The present study reported for the first time, to the best of the authors' knowledge, that the lncRNA SNHG12 is a key coptisine mediator in AS treatment because the depletion of SNHG12 eliminated the protective effect of coptisine on HUVECs.

Consistent with previous reports (30,31), SNHG12 was predominantly located in the cytoplasm of HUVECs, suggesting that this non-coding RNA may regulate downstream targets that act as molecular sponges to adsorb miRNAs. Dual-luciferase and RNA pull-down assays were performed to confirm the interaction between SNHG12 and miR-603 in HUVECs for the first time to the best of the authors' knowledge. In addition, the age-related gene NAMPT, which is involved in NAD(+) regulation, is a direct miR-603 target. This finding is particularly important because NAD(+) and NADH are interconverted in cells and a decrease in NAD(+) levels can lead to mitochondrial dysfunction, increased cellular oxidative stress and reduced DNA repair capacity, resulting in a lower NAD(+)/NADH ratio (32). The dose-dependent increase in NAMPT expression observed following coptisine treatment suggested a potential mechanism through which NAMPT protected HUVECs. Subsequent experiments showed that inhibiting miR-603 expression enhanced the protective effect of coptisine, whereas simultaneous SNHG12 expression suppression counteracted the effect of miR-603. However, these effects were reversed when NAMPT was overexpressed, which is consistent with previous studies that demonstrate NAMPT-induced cellular senescence reduction (33,34). Thus, SNHG12 was found to promote NAMPT expression by inhibiting miR-603, confirming that the SNHG12/miR-603/NAMPT axis was involved in coptisine's protective effect on HUVECs against Ang II-induced decrease in cell viability, increased senescence, apoptosis and inflammation. This is the first evidence that miR-603 affects the growth, apoptosis and cellular senescence of HUVECs.

SIRT3, a member of the sirtuin protein family, exhibits deacetylase activity and requires NAD(+) as a cofactor (35). Elevated NAD(+) levels can enhance SIRT3 activity, leading to deacetylation of p53, a key cellular senescence and apoptosis regulator (36,37). Reduced p53 transcriptional activity inhibited cellular senescence and apoptosis (37). The present study showed that upregulating NAMPT expression mediated NAD(+)'s accelerated synthesis, which promoted SIRT3 activation and p53 deacetylation. Therefore, the SNHG12/miR-603/NAMPT axis is involved in coptisine's protective effects through accelerated NAD(+) synthesis and SIRT3 activation, causing p53 deacetylation and preventing senescence and apoptosis in HUVECs. This molecular axis is activated in response to coptisine, which improves the function of HUVECs.

However, the present study had several limitations. First, the experiments were primarily based on *in vitro* cell models. Future research should verify the therapeutic effects of coptisine on AS animal models. Second, the experiments were performed using HUVECs, which may not fully reflect the complex environment of the vascular system *in vivo*. Third, AngII induces NF-κB activation in HUVEC through the p38MAPK pathway (38); thus, more validation is needed to verify whether flavonoid alkaloids directly inhibit NF-κB and thus reduce inflammation. Fourth, the use of HUVECs is largely based on their wide availability and extensive use in preliminary studies and more accurate characterization employing human coronary artery endothelial cell lines might be preferable, especially in conjunction with 3D culture. Fifth, the performance of HUVECs in the presence of low doses of coptisine was only tested for cell viability and perhaps insufficiently. Finally, clinical trials investigating the treatment of AS using coptisine have not yet been conducted. These issues require further investigation in future research.

In conclusion, the present study contributed to the growing body of evidence highlighting the potential of coptisine as a therapeutic agent for AS and age-related vascular disorders. Identifying the SNHG12/miR-603/NAMPT signaling pathway as a critical mediator of the protective effects of coptisine provided a novel target for future therapeutic interventions and expanded our understanding of the molecular mechanisms underlying vascular homeostasis and dysfunction.

Acknowledgements

Not applicable.

Funding

The present study was supported by the Peak Plateau Subject of Shanghai University of Traditional Chinese Medicine (Special Project for Clinical Talents; grant no. 171319).

Availability of data and materials

The datasets used and/or analyzed during the current study are available from the corresponding author on reasonable request.

Authors' contributions

JM and DL designed the study and developed the methodology. XS and XX conducted the experiments. DL and JC collected and interpreted data. JM and DL drafted the manuscript. All authors read and approved the final manuscript. JM and DL confirm the authenticity of all the raw data.

Ethics approval and consent to participate

Not applicable.

Patient consent for publication

Not applicable.

Competing interests

The authors declare that they have no competing interests.

References

1. Kong P, Cui ZY, Huang XF, Zhang DD, Guo RJ and Han M: Inflammation and atherosclerosis: Signaling pathways and therapeutic intervention. Signal Transduct Target Ther 7: 131, 2022.
2. Libby P: The changing landscape of atherosclerosis. Nature 592: 524-533, 2021.
3. Suzuki K, Susaki EA and Nagaoka I: Lipopolysaccharides and cellular senescence: Involvement in atherosclerosis. Int J Mol Sci 23: 11148, 2022.
4. You Y, Sun X, Xiao J, Chen Y, Chen X, Pang J, Mi J, Tang Y, Liu Q and Ling W: Inhibition of S-adenosylhomocysteine hydrolase induces endothelial senescence via hTERT downregulation. Atherosclerosis 353: 1-10, 2022.
5. Chen L, Qu H, Guo M, Zhang Y, Cui Y, Yang Q, Bai R and Shi D: ANRIL and atherosclerosis. J Clin Pharm Ther 45: 240-248, 2020.
6. Liu Y, Gong S, Li K, Wu G, Zheng X, Zheng J, Lu X, Zhang L, Li J, Su Z, *et al*: Coptisine protects against hyperuricemic nephropathy through alleviating inflammation, oxidative stress and mitochondrial apoptosis via PI3K/Akt signaling pathway. Biomed Pharmacother 156: 113941, 2022.
7. Kim SY, Hwangbo H, Kim MY, Ji SY, Lee H, Kim GY, Kwon CY, Leem SH, Hong SH, Cheong J and Choi YH: Coptisine induces autophagic cell death through down-regulation of PI3K/Akt/mTOR signaling pathway and up-regulation of ROS-mediated mitochondrial dysfunction in hepatocellular carcinoma Hep3B cells. Arch Biochem Biophys 697: 108688, 2021.
8. Suzuki H, Tanabe H, Mizukami H and Inoue M: Differential gene expression in rat vascular smooth muscle cells following treatment with coptisine exerts a selective antiproliferative effect. J Nat Prod 74: 634-638, 2011.
9. Suzuki H, Tanabe H, Mizukami H and Inoue M: Selective regulation of multidrug resistance protein in vascular smooth muscle cells by the isoquinoline alkaloid coptisine. Biol Pharm Bull 33: 677-682, 2010.
10. Xu Z, Feng W, Shen Q, Yu N, Yu K, Wang S, Chen Z, Shioda S and Guo Y: Rhizoma coptidis and berberine as a natural drug to combat aging and aging-related diseases via anti-oxidation and AMPK activation. Aging Dis 8: 760-777, 2017.
11. Cao Q, Wu J, Wang X and Song C: Noncoding RNAs in vascular aging. Oxid Med Cell Longev 2020: 7914957, 2020.
12. Yu XH, Deng WY, Chen JJ, Xu XD, Liu XX, Chen L, Shi MW, Liu QX, Tao M and Ren K: LncRNA kcnq1ot1 promotes lipid accumulation and accelerates atherosclerosis via functioning as a ceRNA through the miR-452-3p/HDAC3/ABCA1 axis. Cell Death Dis 11: 1043, 2020.
13. Haemmig S, Yang D, Sun X, Das D, Ghaffari S, Molinaro R, Chen L, Deng Y, Freeman D, Moullan N, *et al*: Long noncoding RNA SNHG12 integrates a DNA-PK-mediated DNA damage response and vascular senescence. Sci Transl Med 12: eaaw1868, 2020.
14. Ramakrishnan V, Xu B, Akers J, Nguyen T, Ma J, Dhawan S, Ning J, Mao Y, Hua W, Kokkoli E, *et al*: Radiation-induced extracellular vesicle (EV) release of miR-603 promotes IGF1-mediated stem cell state in glioblastomas. EBioMedicine 55: 102736, 2020.
15. Lu J, Wang L, Chen W, Wang Y, Zhen S, Chen H, Cheng J, Zhou Y, Li X and Zhao L: miR-603 targeted hexokinase-2 to inhibit the malignancy of ovarian cancer cells. Arch Biochem Biophys 661: 1-9, 2019.
16. Garten A, Schuster S, Penke M, Gorski T, de Giorgis T and Kiess W: Physiological and pathophysiological roles of NAMPT and NAD metabolism. Nat Rev Endocrinol 11: 535-546, 2015.
17. Abdellatif M, Sedej S and Kroemer G: NAD^+ metabolism in cardiac health, aging, and disease. Circulation 144: 1795-1817, 2021.
18. Cao M, Zhao Q, Sun X, Qian H, Lyu S, Chen R, Xia H and Yuan W: Sirtuin 3: Emerging therapeutic target for cardiovascular diseases. Free Radic Biol Med 180: 63-74, 2022.
19. Yuan L, Yang J, Li Y, Yuan L, Liu F, Yuan Y and Tang X: Matrine alleviates cisplatin-induced acute kidney injury by inhibiting mitochondrial dysfunction and inflammation via SIRT3/OPA1 pathway. J Cell Mol Med 26: 3702-3715, 2022.
20. Xu S, Li L, Wu J, An S, Fang H, Han Y, Huang Q, Chen Z and Zeng Z: Melatonin attenuates sepsis-induced small-intestine injury by upregulating SIRT3-mediated oxidative-stress inhibition, mitochondrial protection, and autophagy induction. Front Immunol 12: 625627, 2021.
21. Zhang Q, Liu XM, Hu Q, Liu ZR, Liu ZY, Zhang HG, Huang YL, Chen QH, Wang WX and Zhang XK: Dexmedetomidine inhibits mitochondria damage and apoptosis of enteric glial cells in experimental intestinal ischemia/reperfusion injury via SIRT3-dependent PINK1/HDAC3/p53 pathway. J Transl Med 19: 463, 2021.
22. Barjaktarovic Z, Kempf SJ, Sriharshan A, Merl-Pham J, Atkinson MJ and Tapio S: Ionizing radiation induces immediate protein acetylation changes in human cardiac microvascular endothelial cells. J Radiat Res 56: 623-632, 2015.
23. Livak KJ and Schmittgen TD: Analysis of relative gene expression data using real-time quantitative PCR and the 2(-Delta Delta C(T)) method. Methods 25: 402-408, 2001.
24. Navas LE and Carnero A: NAD^+ metabolism, stemness, the immune response, and cancer. Signal Transduct Target Ther 6: 2, 2021.
25. O'Donoghue ML, Giugliano RP, Wiviott SD, Atar D, Keech A, Kuder JF, Im K, Murphy SA, Flores-Arredondo JH, López JAG, *et al*: Long-term evolocumab in patients with established atherosclerotic cardiovascular disease. Circulation 146: 1109-1119, 2022.
26. Bytyçi I, Penson PE, Mikhailidis DP, Wong ND, Hernandez AV, Sahebkar A, Thompson PD, Mazidi M, Rysz J, Pella D, *et al*: Prevalence of statin intolerance: A meta-analysis. Eur Heart J 43: 3213-3223, 2022.
27. Zhang X, Qin Y, Ruan W, Wan X, Lv C, He L, Lu L and Guo X: Targeting inflammation-associated AMPK//Mfn-2/MAPKs signaling pathways by baicalein exerts anti-atherosclerotic action. Phytother Res 35: 4442-4455, 2021.
28. Dörffel Y, Franz S, Pruss A, Neumann G, Rohde W, Burmester GR and Scholze J: Preactivated monocytes from hypertensive patients as a factor for atherosclerosis? Atherosclerosis 157: 151-160, 2001.

29. Liu B, Piao X, Niu W, Zhang Q, Ma C, Wu T, Gu Q, Cui T and Li S: Kuijieyuan decoction improved intestinal barrier injury of ulcerative colitis by affecting TLR4-dependent PI3K/AKT/NF-κB oxidative and inflammatory signaling and gut microbiota. Front Pharmacol 11: 1036, 2020.
30. Yang HG, Wang TP, Hu SA, Hu CZ, Jiang CH and He Q: Long non-coding RNA SNHG12, a new therapeutic target, regulates miR-199a-5p/Klotho to promote the growth and metastasis of intrahepatic cholangiocarcinoma cells. Front Med (Lausanne) 8: 680378, 2021.
31. Qian W, Zheng ZQ, Nie JG, Liu LJ, Meng XZ, Sun H, Xiao FM and Kang T: LncRNA SNHG12 alleviates hypertensive vascular endothelial injury through miR-25-3p/SIRT6 pathway. J Leukoc Biol 110: 651-661, 2021.
32. Covarrubias AJ, Perrone R, Grozio A and Verdin E: NAD^+ metabolism and its roles in cellular processes during ageing. Nat Rev Mol Cell Biol 22: 119-141, 2021.
33. Yang L, Shen J, Liu C, Kuang Z, Tang Y, Qian Z, Guan M, Yang Y, Zhan Y, Li N and Li X: Nicotine rebalances NAD^+ homeostasis and improves aging-related symptoms in male mice by enhancing NAMPT activity. Nat Commun 14: 900, 2023.
34. Gong H, Chen H, Xiao P, Huang N, Han X, Zhang J, Yang Y, Li T, Zhao T, Tai H, *et al*: miR-146a impedes the anti-aging effect of AMPK via NAMPT suppression and NAD^+/SIRT inactivation. Signal Transduct Target Ther 7: 66, 2022.
35. Diao Z, Ji Q, Wu Z, Zhang W, Cai Y, Wang Z, Hu J, Liu Z, Wang Q, Bi S, *et al*: SIRT3 consolidates heterochromatin and counteracts senescence. Nucleic Acids Res 49: 4203-4219, 2021.
36. Nahálková J: Focus on molecular functions of anti-aging deacetylase SIRT3. Biochemistry (Mosc) 87: 21-34, 2022.
37. Yan P, Li Z, Xiong J, Geng Z, Wei W, Zhang Y, Wu G, Zhuang T, Tian X, Liu Z, *et al*: LARP7 ameliorates cellular senescence and aging by allosterically enhancing SIRT1 deacetylase activity. Cell Rep 37: 110038, 2021.
38. Guo RW, Yang LX, Li MQ, Liu B and Wang XM: Angiotensin II induces NF-kappa B activation in HUVEC via the p38MAPK pathway. Peptides 27: 3269-3275, 2006.